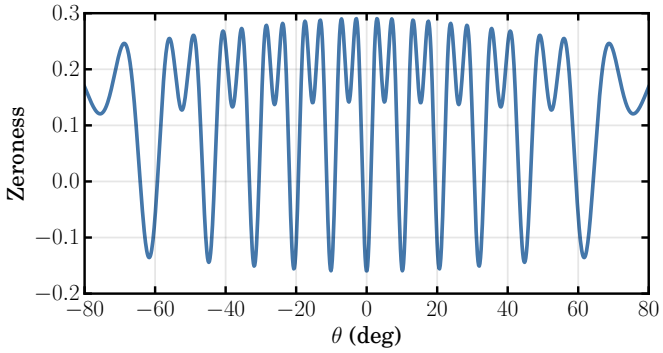

Supplementary Figure 1: Plot of the normalized Sorkin parameter, κ, assuming experimental parameters similar to those used in the main text.

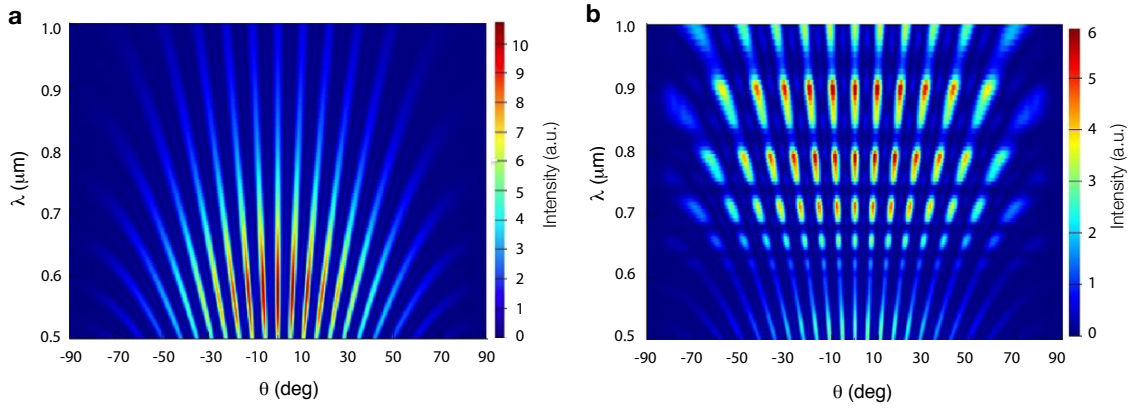

Supplementary Figure 2: The wavelength-dependent intensity distribution of the interference pattern for a three-slit experiment in the absence (**a**) and pretense (**b**) of looped trajectories. Looped trajectories are enhanced by using along the short direction of the slit.

1 Supplementary Note 1: Model

As described in the main text, the path integral formulation of the wave equation propagation kernel is given by

$$K(\mathbf{r}_1, \mathbf{r}_2) = \int \mathcal{D}[x(\mathbf{s})] \exp\left(ik \int \mathrm{d}\mathbf{s}\right), \tag{1}$$

and can be perturbatively expanded as [1]

$$K = K_1 + K_2 + K_3 + \cdots, \tag{2}$$

where K_n represents the nth application of of the Fresnel-Huygens principle. For instance, considering the propagation through the slits from the source located at $\mathbf{r_s}$ to the detector at $\mathbf{r_d}$, the expression for K_2 would be given by

$$K_2(\mathbf{r_s}, \mathbf{r_d}) = \int_\Omega \mathrm{d}\mathbf{r_1} \int_\Omega \mathrm{d}\mathbf{r_2} K(\mathbf{r_s}, \mathbf{r_1}) K(\mathbf{r_1}, \mathbf{r_2}) K(\mathbf{r_2}, \mathbf{r_d}), \tag{3}$$

where integration is over the slit areas Ω. Furthermore, assuming that the slits are much smaller than the wavelength, we can rewrite this equation as a discrete sum over paths. In this case, the expression above becomes

$$K_2(\mathbf{r_s}, \mathbf{r_d}) \approx \sum_{j,k} K(\mathbf{r_s}, \mathbf{r_j}) K(\mathbf{r_j}, \mathbf{r_k}) K(\mathbf{r_k}, \mathbf{r_D}), \tag{4}$$

which represents propagation from the source $\mathbf{r_s}$, to slit j at $\mathbf{r_j}$, and then from slit j to k at $\mathbf{r_k}$, and then finally propagation to the detector at $\mathbf{r_d}$.

Each term in Eq. (4) represents a simple propagation solution. Assuming that the slits are illuminated with a planewave normally incident onto the surface of the slits, then the propagation from the source to the screen is

$$K(\mathbf{r_s}, \mathbf{r_A}) = K(\mathbf{r_s}, \mathbf{r_B}) = K(\mathbf{r_s}, \mathbf{r_C}) = \text{constant}, \tag{5}$$

and the three straight paths in the (paraxial) far field will be given by

$$\begin{aligned} K(\mathbf{r_B}, \mathbf{D}) &\propto \operatorname{sinc}\left(\frac{k_x w}{2\pi}\right) \\ K(\mathbf{r_A}, \mathbf{D}) &= K(\mathbf{r_B}, \mathbf{D}) e^{i\phi_f} \\ K(\mathbf{r_C}, \mathbf{D}) &= K(\mathbf{r_B}, \mathbf{D}) e^{-i\phi_f}, \end{aligned} \tag{6}$$

where θ is the far field angle in the (x, z) plane ($\theta = 0$ corresponding to propagation in the z direction), w is the slit size, p is the spacing between slits, $k_0 = 2\pi/\lambda$ is the free-space wavenumber, $k_x = k_0 \sin(\theta)$ is the transverse wavenumber, and $\phi_f = pk_x$ is the phase difference due to differences in the distance between each slit and the far field.

For the case at hand, the looped paths involve an enhancement of the near field by surface plasmon modes which we solve for via numerical simulations using the FDTD method. For the simple configuration of slits in a metal screen, it has been shown that this is well approximated by the simple input-output relations [2]

$$\begin{aligned} K(\mathbf{r_A}, \mathbf{r_B}) = K(\mathbf{r_B}, \mathbf{r_A}) = K(\mathbf{r_B}, \mathbf{r_C}) = K(\mathbf{r_C}, \mathbf{r_B}) = a e^{i\phi_{\mathrm{SP}}} \\ K(\mathbf{r_A}, \mathbf{r_C}) = K(\mathbf{r_C}, \mathbf{r_A}) = b e^{i2\phi_{\mathrm{SP}}}, \end{aligned} \tag{7}$$

where a and b are the relevant field strengths quantifying the coupling of a free-space to surface plasmon back to free-space mode for neighboring slits and paths with an extra slit between, and $\phi_{\mathrm{SP}} = k_{\mathrm{SP}} p$ is the phase accumulated along the plasmon path between slits.

A plot of the normalized Sorkin parameter, κ, is shown in Supplementary Figure 1 assuming the parameters $p = 4.6\,\mu\text{m}$, $w = 200\,\text{nm}$, and $\lambda = 810\,\text{nm}$, equivalent to the main paper. This plot was generated using the surface plasmon mode coupling parameters $a = 2b = 0.3$, and $k_{\text{SP}} = 1.65k_0$. When this plot is compared with Supplementary Figure 1 in the main document, it can be seen that this simple model matches the observed features in both the experiment and full FDTD simulations of the experiment.

2 Supplementary Note 2: Signs of Looped Trajectories

Since the exotic looped trajectories of light are intimately related to the evanescent component of the fields, the conditions under which the probability of photons following looped trajectories are increased depends on the characteristics of the three slits and the physical processes that take place in their vicinity. The most suitable characteristics for the slits were found by investigating the regimes under which the looped trajectories show a significant role in the formation of interference fringes. We carried out this task by performing a series of FDTD simulations in which different slit sizes, slit separations, and metal thickness were studied.

In Supplementary Figure 2 we show distinct interference structures that unveil the importance of looped trajectories in the formation of interference structures. We plot the intensity as a function of wavelength and detector angles, or positions in the far-field of the three slits. In our calculations, we consider that the slits have a width of $w = 150$ nm, the separation between slits is $p = 3.6\mu$m, the hight of the slits is infinite, and the three-slit structure is illuminated by a planewave at normal incidence. We show two interference structures produced by the same three-slit structure but under different illumination conditions. When these slits are illuminated with light polarized along the long axis of the slits, surface plasmon modes are not excited in the structure and the interference pattern shown in Supplementary Figure 2a is shown in the far field. This pattern is practically identical to that obtained by simply applying the Fourier transform of the three slits. However, this simple experiment shows a striking interference structure when the slits are illuminated with light polarized along the short axis of the slits. In this case, surface plasmon modes are efficiently excited, leading to an increased probability for looped paths, which in turn leads to the significantly different interference pattern shown in Supplementary Figure 2b. In addition, from this pattern it is quite clear how interference effects among looped trajectories lead to a clear wavelength dependence of the experiment.

The remarkable difference between these two interference structures offered us a clear signature of the presence of looped trajectories. We used this knowledge to decide the characteristics of the slits and the conditions we used when we performed the experiment.

Supplementary references

[1] R. Sawant, J. Samuel, A. Sinha, S. Sinha, and U. Sinha, "Nonclassical Paths in Quantum Interference Experiments," *Phys. Rev. Lett.*, vol. 113, p. 120406, Sept. 2014.

[2] H. F. Schouten, N. Kuzmin, G. Dubois, T. D. Visser, G. Gbur, P. F. A. Alkemade, H. Blok, G. W. Hooft, D. Lenstra, and E. R. Eliel, "Plasmon-Assisted Two-Slit Transmission: Youngs Experiment Revisited," *Phys. Rev. Lett.*, vol. 94, p. 053901, feb 2005.